Power System Dynamic Performance During the Late-Time (E3) High-Altitude Electromagnetic Pulse

Trevor R. Hutchins and Thomas J. Overbye

University of Illinois at Urbana-Champaign: Dept. of Electrical and Computer Engineering
Urbana, Illinois, USA
hutchns2@illinois.edu, overbye@illinois.edu

Abstract--**A high altitude electromagnetic pulse (HEMP) has the potential to cripple power systems. A HEMP is a nuclear detonation, occurring at least 30 km above the surface of the earth. HEMPs emit harmful radiation in the form of electromagnetic waves. A HEMP can be broken down into three energetic waves, realized as geoelectric fields, E1, E2 and E3. This paper focuses on the impacts of HEMP E3 to power systems. Provided by the International Electrotechnical Commission for unclassified use is a single HEMP E3 reference field. The E3 field could be prone to slight variations due to various atmospheric conditions and weapon characteristics. As a result, studying the impacts of one specific field may be incomplete. In this paper, slight variations to the referenced field are made in order to better understand the potential power system impacts and sensitivities to various geoelectric field characteristics. The results show that the system's response is the most sensitive to changes to the geoelectric field's magnitude.**

Index Terms—**Geomagnetically Induced Current (GIC), High Altitude Electromagnetic Pulse (HEMP), transient stability**

I. INTRODUCTION

The power system impacts of HEMP E3 are very similar to those of geomagnetic disturbances (GMDs); however key characteristics require the two to be studied differently. Currently, HEMP E3 and GMD research are often lumped together. HEMP E3 is similar to GMDs in the sense that they both produce geomagnetically induced current (GIC). GIC is a slow varying, dc current that enters and leaves power systems through wye grounded transformers. GIC is driven by geoelectric fields. The geoelectric field, $\bar{E}$, is the result of slow fluctuations in the earth's magnetic field. In line dc voltages, V_{dc}, are then induced via Faraday's Law, and are modeled in the transmission lines, calculated according to (1), [1].

$$V_{dc} = \oint_{\Sigma} \bar{E} \cdot d\bar{l} \qquad (1)$$

$d\bar{l}$ is the incremental distance along the path of the transmission line, Σ. Next, the dc bus voltages, $\mathbf{V}$, of the system are calculated by solving Ohm's law [2] [3],

$$\mathbf{V} = \mathbf{G^{-1}I} . \qquad (2)$$

The inline dc line voltages, are transformed into their Norton equivalents and are represented by the current injection vector, $\mathbf{I}$. The power network's conductance values are comprised in the square matrix, $\mathbf{G}$.

$\mathbf{G}$ is similar in form to the power flow admittance matrix, except it is purely real and it is augmented to include substation ground resistance values as well as substation neutral buses.

The elements of $\mathbf{G}$ are three phase values, determined by the three phase parallel combination of the line resistances. Given branch resistances, the GIC in any branch can then be calculated, with the system's dc bus voltages known.

GICs are known to have caused large scale power outages, lasting as long as nine hours, such as the collapse of the Quebec grid [4]. GICs can saturate high voltage transformers, increasing the reactive power demand on the system, ultimately jeopardizing the voltage stability of the system [5]. The GMD problem is framed in the steady state domain since the disturbances have rise-times on the order of minutes to hours. HEMP E3 has rise-times on the order of a few seconds, making it more appropriate for transient stability analysis.

A HEMP generates two other electromagnetic waves known as E1 and E2. These waves have rise-times on the order of nanoseconds and microseconds, respectively. More about these waves, and their impacts to power systems is found in [6].

HEMP E3 can be realized as a geoelectric field. Several parameters impact the resulting characteristics of the induced geoelectric field. Geoelectric field characteristics such as, rise-time, duration, and magnitude can all be affected by the weapon yield/makeup, detonation altitude, and ionospheric conductivity structure [7]. As a result, slightly varying geoelectric fields could be induced. As a primary reference, a HEMP E3 geoelectric field has been provided in IEC-61000-2-9 [8]. Many details behind the exact field remain classified. Due to uncertainties or adversarial desires, the wave could take on slightly different forms. For example, the weapon could be optimized to induce a geoelectric field with a faster rise-time and of longer duration. A power system's responses to various geoelectric fields are studied and compared in this paper.

This paper is organized as follows. Section II describes the background of how HEMP E3 is included into transient stability analysis. Section III describes the test case used for the simulations, as well as the geoelectric fields used. Section IV contains the results and Section V is the Summary and Future Work.

II. BACKGROUND

The power system transient stability power balance model can be augmented to include the increased reactive power demand of the GIC saturated transformers. The additional reactive power loss varies linearly with GIC and the bus voltage and hence, it is modeled as a constant current reactive load [9] [10]. The additional reactive power loading can be expresses as,

$$Q_{Loss,pu} = V_{pu}KI_{GIC,pu} . \qquad (3)$$

$Q_{Loss,pu}$ is the reactive power loss in per unit due to the GIC saturated transformer, V_{pu} is the high side ac terminal bus voltage in per unit, K is a transformer-type specific, dimensionless scalar, and $I_{GIC,pu}$ is the effective GIC, in per unit, flowing through the transformer. It is called 'effective' GIC because the actual GIC is adjusted in order to account for the transformer specific parameters. Together, K and $I_{GIC,pu}$ account for the differences of how a transformer behaves during core saturation, its winding configuration, and its facilitation of neutral current flow [11].

The additional reactive power loading is then incorporated into the power system transient stability model. The transient stability model is a set of differential algebraic equations of the form,

$$\dot{\mathbf{x}} = f\left(\mathbf{x}, \mathbf{y}\right) \tag{4}$$

$$0 = g\left(\mathbf{x}, \mathbf{y}\right). \tag{5}$$

Where (4) represents the dynamics of the system with differential equations, and (5) are the network and stator algebraic equations [12]. The dynamic state variables are contained in $\mathbf{x}$, and the power flow state variables such as bus voltage and angle are in $\mathbf{y}$. The equations are governed by the power system network as well as the dynamic models used in the simulation.

The GIC reactive power loading, (3), is incorporated into the network algebraic equations of (5). Numerical integration schemes are used to solve (4) and (5) for the states. During the solution process (2) needs to be solved at each time step and $Q_{Loss,pu}$ updated and included in the reactive power balance equations of (5). However, since $\mathbf{G}$ is does not need to be refactored, this only requires a forward/backward substitution. The updated reactive power balance equations with the inclusion of the GIC reactive power loading, are shown in (6) and (7).

$$Q_{Gen,i} + Q_{L,i} + Q_{Loss,i} - \sum_{k=1}^{n} V_i V_k Y_{ik} \sin\left(\theta_i - \theta_k - \alpha_{ik}\right) = 0, i = 1,...,m \tag{6}$$

$$Q_{L,i} + Q_{Loss,i} - \sum_{k=1}^{n} V_i V_k Y_{ik} \sin\left(\theta_i - \theta_k - \alpha_{ik}\right) = 0, i = m+1,...,n \tag{7}$$

Since a load can be present at a generator bus or a load bus, the reactive power balance equations are shown for each, respectively. $Q_{L,i}$, from (6) and (7), is the reactive load at bus i, $Q_{loss,i}$ is the transformer reactive power loss due to GIC at bus i, from (3). Note that $Q_{loss,i}$ is calculated and accounted for at each bus i if bus i is the high-side terminal bus of a transformer, otherwise $Q_{Loss,i}$ is zero. $Q_{Gen,i}$ is the reactive power supplied by the generator at bus i. V_i is the voltage at bus i. Y_{ik} and α_{ik} are the admittance and admittance angle, respectively, between buses i and k. The bus angle is given by θ. m is the number of generator buses whereas n is the total number of buses in the system. The real power network equations are not shown here, since the loading on the transformers due to GIC is strictly reactive.

III. CASE STUDIES

An example system covered in the paper is a 42 bus case which contains a full system dynamic model. The network consists of 161 kV, 345 kV, and 500 kV buses. The system will be exposed to slight variations of the IEC geoelectric field. These different fields could result in drastically different power system responses. This hypothesis will be put to the test by making small changes to the IEC geoelectric field such as slightly adjusting its rise-time, duration, and/or magnitude.

A. Test Case

The test case that will be subjected to the disturbances is an adaptation of the 20 bus GIC benchmark case found in [13]. The 20 bus case has been augmented to include dynamic models for the loads, generators, exciters, and governors. The case also has basic protection systems modeled in the form of over excitation limiters (OELs), load relays, generator relays, and line relays. The inclusion of the protection system in transient stability modeling for HEMP E3 analysis is vital to the dynamic response of the system. Frequency constraints on the system are imposed through the use of generator relays but are somewhat relaxed compared to typical frequency restrictions. The generator relays are configured to trip if the frequency deviates beyond 3% for more than 5 seconds. Most of the load has been moved to a new 161 kV network, which has been added to the case. GIS information, as well as ac line parameter data has been added to the case in order to make it appropriate for GIC transient stability analysis [14]. A constant impedance load model is used for the entire load, throughout each simulation. Although it is not the focus of this paper, it is possible that low cost mitigation strategies could be developed by configuring protection systems appropriately for HEMP E3. Fig. 1 shows a snapshot of the 42 bus system.

B. Geoelectric Fields

Four different potential HEMP E3 geoelectric fields were imposed on the 42 bus system. These fields were developed arbitrarily by slightly perturbing the reference IEC field. The fields are shown in Fig. 2, and all assume a uniform ground conductivity.

1) IEC – reference HEMP E3 composite geoelectric field provided by the IEC

2) Fast Rise – geoelectric field is identical to 1) except the field rises four times as fast

3) Fast and High – geoelectric field rises and falls four times as fast and has an increased magnitude of 1.44 times 1)

4) Slow and Low – geoelectric field rises four times slower and reaches a peak magnitude of 0.625 times 1)

The IEC does not provide spatial data for the geoelectric field. In order to simulate the effects of the weapon's spatial distribution, each field was imposed on the system, scaled to 40%, 70%, and 100% of its peak field value.
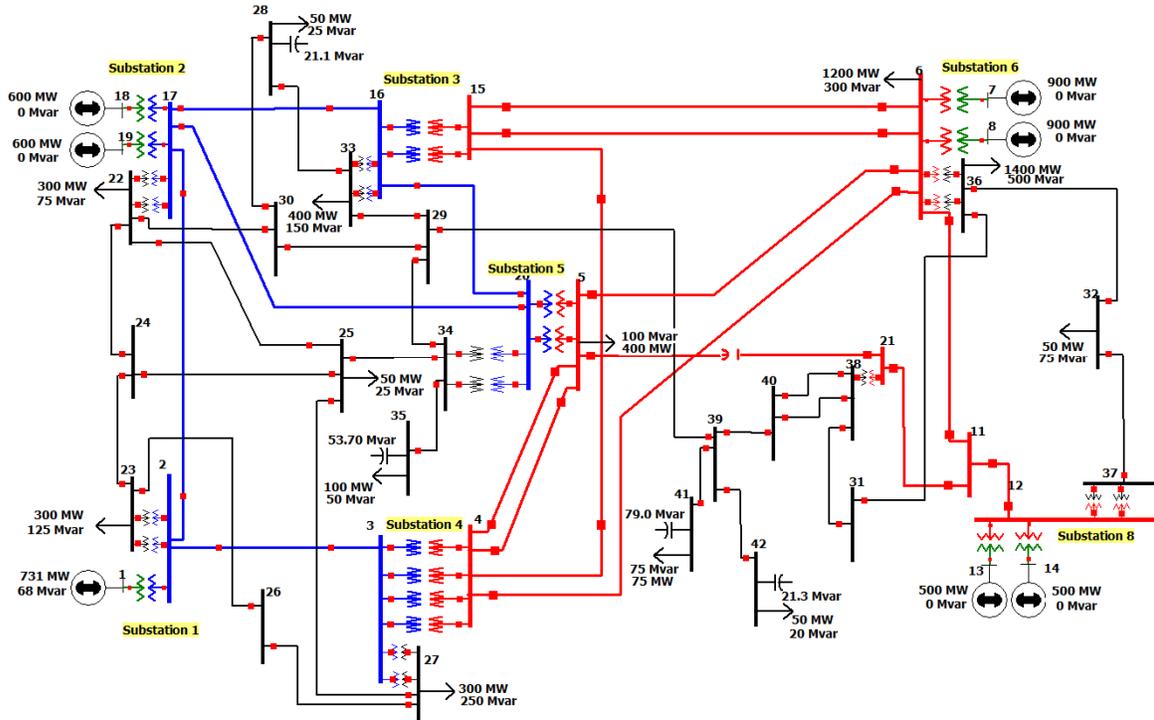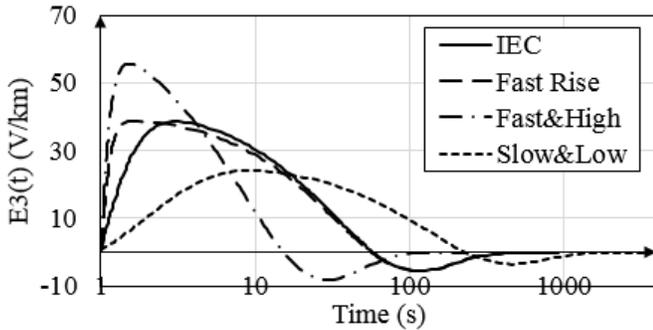
Fig. 1. 42 bus test case

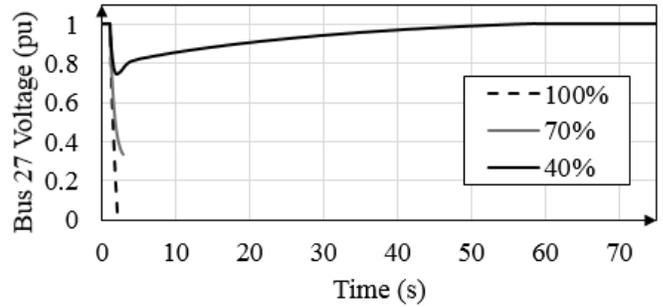Fig. 2. Geoelectric fields used for simulations, 100% scaling

Fig. 3. System response to the IEC reference geoelectric field

It is very possible that the power network may lie in a region that is not in the most intense area of the geoelectric field. Depending on the blast location and altitude, it is possible that most power networks could be in regions that experience significantly attenuated geoelectric fields.

The area exposed to the 100% geoelectric field could be much less than the area exposed to less than 40% intensity [7]. It is also possible that large networks could span multiple areas of intensity. For this paper, it is assumed the power network is small enough that it does not span multiple areas. In order to simulate the power network lying in entirely different geoelectric field intensity areas, the disturbances are scaled and separate simulations are run for each scaled disturbance.

IV.   RESULTS

A. IEC Reference Geoelectric Field

The first 60 seconds of the IEC reference geoelectric field was applied to the test case. After the first 60 seconds, the field

has negligible magnitude and is not changing fast enough to significantly impact the system dynamics, therefore it is not simulated. The lowest bus voltage of the system response is shown for each geoelectric field intensity in Fig. 3. The system quickly collapses due to non-convergence for the 100% and 70% cases.

The reactive power demand is too significant for the system to recover. Without change to the temporal evolution of the field, it is not surprising that the higher intensity fields negatively impact the power system more than the 40% field. The system recovers from the 40% intensity field without loss of load. The system experiences a voltage drop, dipping as low as 0.745 pu. Protection systems did not trigger since the states did not violate any of the protection system settings.

B. Fast Rise

A faster rising geoelectric field could pose as an increased threat to the short-term voltage stability of the power system. The fast rise field rises four times faster than the reference IEC
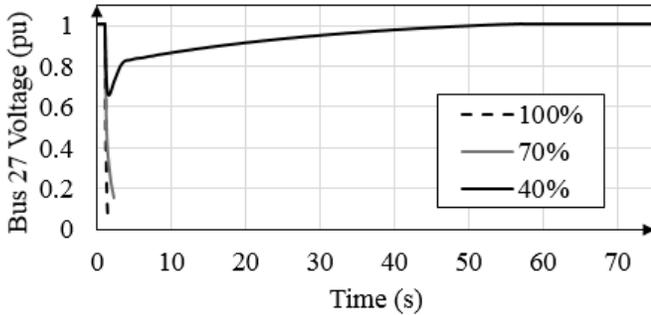
Fig. 4. System response to the fast rising geoelectric field

field but decays at the same rate as the reference field. The simulation results are shown in Fig. 4. The faster rising field results in the system suffering a larger voltage drop at the most intense part of the disturbance, compared to that of the IEC reference scenario. The system fails in a similar fashion to that of the reference field for the 100% and 70% field intensity scenarios.

However, the 40% field intensity scenario recovers without the loss of any load, despite the disturbance's rise-time being four times that of the reference field.

C. Fast and High

The fast and high geoelectric field rises and falls four times as fast as the reference field. It also is larger in magnitude by a factor of 1.44. The fast and high disturbance last about 160 seconds with non-negligible magnitude, therefore the entire disturbance is simulated. The simulation results are shown in Fig. 5.

The fast and high geoelectric field had the most impact to the power system, at all levels of intensity, when compared to the other IEC perturbed fields. The 100% and 70% scenarios resulted in a non-convergence immediately as the disturbance began. The system was able to maintain stability for the 40% scenario, however it did so by shedding load. The undervoltage load relays triggered on buses 5, 27, and 33 according to their relay settings of being lower than 0.75 pu for more than 2 seconds. Between 3.1 and 3.129, 1230 MVA was shed, or about ¼ of the system load. After the load was shed, and the disturbance began to decay, and the system settled into a new steady state operating point with slightly higher bus voltages, since ¼ of the load remained offline.
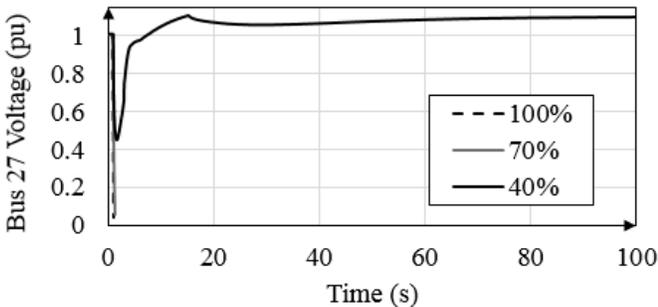

Fig. 5. System response to the fast and high rising geoelectric field

D. Slow and Low

As expected, the slow and low geoelectric field had the least impact to the short term voltage stability of the power system for all field intensity scenarios. The disturbance changes slowly enough that most of it is outside of the time response of the dynamics of the power system. However, the geoelectric field has a higher sustained geoelectric field than all of the others. The first 230 seconds of the geoelectric field was modeled into the simulations to catch any longer term protection violations that would not have occurred for the other geoelectric fields. The simulation results are shown in Fig. 6.
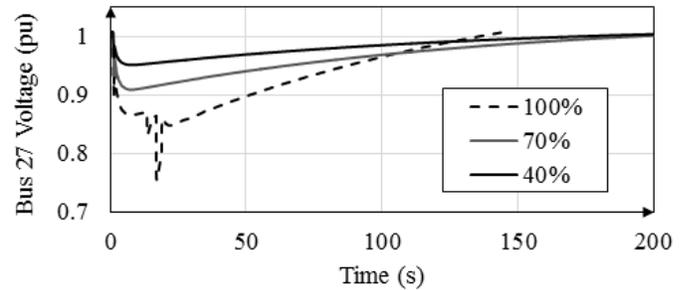

Fig. 6. System response to the slow and low rising geoelectric field

The first protections system action performed in the 100% field intensity scenario is the opening of generator 18 by an overexcitation relay at 13.65 seconds. A few seconds thereafter, a series of loads trips, followed by the remaining generators tripping at 144 seconds. The sustained geoelectric field proved to be too great for the system to maintain convergence. This is similar to how a system would fail due to a GMD, in the sense that the system cannot keep up with the additional load over time [5]. For the 70% intensity scenario, the lowest experienced voltage was 0.84 pu, no load was tripped, and the system returned to its original operating point. It should be noted that even though no load was shed, the system voltages were depressed longer than any of the other reference field perturbations. The system response to the 40% intensity scenario was very similar to that of the 70%. The 40% intensity scenario experienced a voltage as low as 0.92 pu. The slow and low field scenarios were the most forgiving to the system dynamics. Since the fields varied so slowly, the dynamics of the system were able to keep up with the changes imposed by the disturbances. Also aiding in the robustness of the system response, compared to the other field perturbations, was the lower field magnitude.

E. 40% Comparison

In order to directly compare the system responses to the various geoelectric fields more easily, the system responses to each 40% intensity field are shown together in Fig. 7. The system responses to the fast rise and IEC reference field are very similar. The most unique system responses are the responses to the slow and low geoelectric field and the fast and high geoelectric field, pointing towards the observation that a change in geoelectric field magnitude greatly impacts the system response. This is also observed by comparing the

system responses to different field intensities of a specific geoelectric field.

V. SUMMARY AND FUTURE WORK

This paper compared and studied the responses of a 42 bus power system subjected to potential HEMP E3 geoelectric fields. By applying perturbations to the IEC reference geoelectric field, sensitivities of certain field parameters were studied.

It was shown that the system's response was most sensitive to changes to the geoelectric field's magnitude. Varying the rise and decay time of the field did impact the system response, but not to the extent that varying the magnitude did. How the system responds is very dependent on the dynamic models and protection system settings used in the power system model. The models and setting used in this paper are popular choices in transient stability studies, with the exception of the relaxed frequency constraints. The impacts of E1 and E2 were not considered in this work, but were considered in [6]. It is possible portions of the load would become damaged and drop before the E3 wave strikes, potentially impacting the dynamic response of the system.

One extension of this work could be studying how neighboring power systems contribute to voltage stability during HEMP E3 disturbances. Neighboring power systems may be in higher or lower geoelectric field intensity areas, hence contributing or distributing the burden of reactive power loading to the network of interest. Similar research has been performed in the GMD domain, studying how sensitive GICs for individual transformers are to the assumed geoelectric field on the transmission lines [15]. These large system studies present research challenges, such as modeling the spatial distribution of the geoelectric fields as well as the incorporation of ground conductivity models.
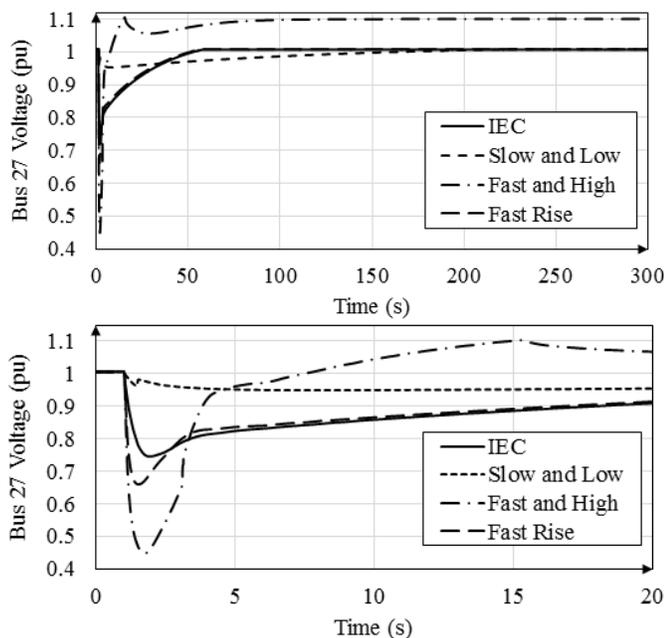

Fig. 7. Comparisons of the system response to 40% field intensities

Delivering software that is capable of simulating the effects of HEMP E3to power systems to the hands of power system operators and planners is a crucial step in the hopes of mitigating the threat. Planners and operators intimately know their systems and can better create mitigation strategies.

HEMP E3 analysis belongs in the transient stability domain. Its faster rise-times, on the order of seconds, separates it from steady state GMD analysis. This paper focused on the voltage response of the system. The frequency response of the system is also of importance, but not the focus of this paper. One of the many challenges of incorporating HEMP E3 into transient stability analysis is identifying the appropriate load models. This paper assumes a constant impedance load model for the load. In reality, the load has dynamics associated with it as well, but can be very power system dependent. Power system operators and planners would be able to characterize their load more appropriately when performing studies such as these in an effort to mitigate the risks associated with HEMP E3.

REFERENCES

[1] D. H. Boteler and R. J. Pirjola, "Modeling Geomagnetically Induced Currents Produced by Realistic and Uniform Electric Fields," *IEEE Transactions on Power Delivery,* vol. 13, pp. 1303-1308, Oct 1998.

[2] V. D. Albertson, J. G. Kappenman, N. Mohan and G. A. Sharbakka, "Load=Flow Studies in the Presence of Geomagnetically-Induced Currents," *IEEE Transactions on Power Apparatus and Systems,* vol. 100, pp. 594-606, February 1981.

[3] T. J. Overbye, T. R. Hutchins, K. S. Shetye, Y. Z. Hughes, J. D. Weber and S. Dahman, "Integration of Geomagnetic Disturbance Modeling into the Power Flow: A methodology for Large-Scale Sysstem Studies," in *North American Power Symposium*, Champaign, IL, September 2012.

[4] J. G. Kappenman and V. D. Albertson, "Bracing for the geomagnetic storms," *IEEE Spectrum,* pp. 27-33, March 1990.

[5] T. J. Overbye, K. S. Shetye, Y. Z. Hughes and J. D. Weber, "Preliminary Consideration of Voltage Stability Impacts of Geomagnetically Induced Currents," in *Power and Energy Society General Meeting (PES)*, July 2013.

[6] T. R. Hutchins, "Modeling, simulation, and mitigation of the impacts of the late time (E3) high altitude electromagnetic pulse on power systems," PhD dissertation, Dept of Elect. and Comp. Eng., Univeristy of Illinois at Urbana-Champaign, Urbana, IL, Nov 2015.

[7] Metatech Coporation, "The Late-Time (E3) High-Altitude Electromagnetic Pulse (HEMP) and Its Impact on the U.S. Power Grid," Oak Ridge National Laboratory, January 2010.

[8] "Electromagnetic compatibility (EMC) – Part 2: Environment – Section 9: Description of HEMP environment – Radiated disturbance. Basic EMC publication," International Electrotechnical Commission, Geneva, Switzerland, 1996.

[9] V. D. Albertson, J. M. Thorson Jr., R. E. Clayton and S. C. Tripathy, "Solar-Induced-Currents in Power Systems: Cause and Effects," *IEEE Transactions on Power Appartus and Systems,* vol. 92, no. 2, pp. 471-477, April 1973.

[10] R. A. Walling and A. H. Khan, "Characteristics of Transformer Exciting Current During Geomagnetic Disturbances," *IEEE Transactions on Power Delivery,* vol. 6, no. 4, October 1991.

[11] X. Dong, Y. Liu and J. G. Kappenman, "Comparitive Analysis of Exciting Current Harmonics and Reactive Power Consumption from GIC Saturated Transformers," in *IEEE 2001 Winter MEeting*, Columbus, OH, Jan 2001.

[12] P. W. Sauer and M. A. Pai, Power System Dynamics and Stability, Champaign, IL: Stripes Publishing LLC, 1997.

[13] R. Horton, D. H. Boteler, T. J. Overbye, R. Pirjola and R. C. Dugan, "A Test Case for the Calculation of Geomagnetically Induced Currents," *IEEE Transactions on Power Systems,* vol. 27, no. 4, pp. 2368-2373, October 2012.

[14] T. R. Hutchins, "42 Bus HEMP E3 Case," [Online]. Available: http://publish.illinois.edu/smartergrid/illinigmd-42-hemp/.

[15] T. J. Overbye, S. K. Shetye, T. R. Hutchins, Q. Qiu and J. D. Weber, "Power Grid Sensitivity Analysis of Geomagnetically Induced Currents," *IEEE Transactions on Power Systems,* vol. 28, no. 4, pp. 4821-4828, November 2013.